Stem Cell Reports, Volume *17*

Supplemental Information

Homozygous ALS-linked *FUS* P525L mutations cell- autonomously perturb transcriptome profile and chemoreceptor signaling in human iPSC microglia

Sze Yen Kerk, Yu Bai, Janell Smith, Pranav Lalgudi, Charleen Hunt, Junko Kuno, John Nuara, Tao Yang, Kathryn Lanza, Newton Chan, Angel Coppola, Qian Tang, Jennifer Espert, Henderson Jones, Casey Fannell, Brian Zambrowicz, and Eric Chiao

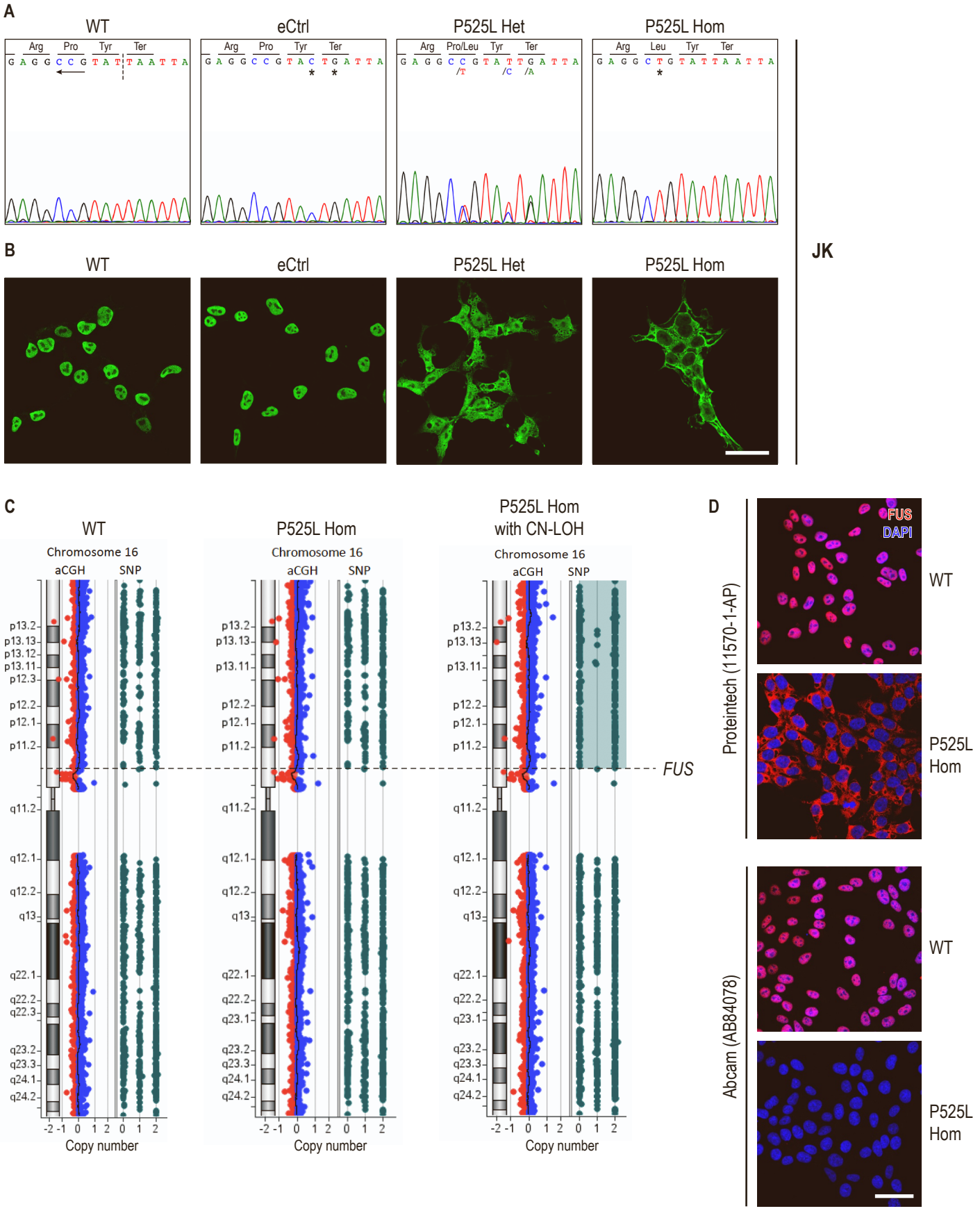
A
WT
eCtrl
P525L Het
P525L Hom
Arg Pro Tyr Ter
G A G G C C G T A T T A A T T A
Arg Pro Tyr Ter
G A G G C C G T A C T G A T T A
Arg Pro/Leu Tyr Ter
G A G G C C G T A T T G A T T A
/T /C /A
Arg Leu Tyr Ter
G A G G C T G T A T T A A T T A
B
WT
eCtrl
P525L Het
P525L Hom
JK
C
WT
P525L Hom
P525L Hom with CN-LOH
Chromosome 16
aCGH
SNP
p13.2
p13.13
p13.12
p13.11
p12.3
p12.2
p12.1
p11.2
q11.2
q12.1
q12.2
q13
q22.1
q22.2
q22.3
q23.1
q23.2
q23.3
q24.1
q24.2
FUS
-2 -1 0 1 2 0 1 2
Copy number
D
Proteintech (11570-1-AP)
Abcam (AB84078)
FUS
DAPI
WT
P525L Hom
WT
P525L Hom

Figure S1. CRISPR engineering of *FUS* P525L mutations and isogenic controls in independent human iPSC lines. Related to Figure 1.

(A) Sanger sequencing of CRISPR-engineered *FUS* genomic locus in human iPSC lines. In the WT panel, the inverted NGG PAM site is underlined by the arrow whereas the Cas9 endonuclease cut site is bisected by the perforated line. Homozygous point mutations compared to WT, such as that in P525L Hom, are denoted by asterisks (*). Heterozygous point mutations such as those in P525L Het are denoted by a slash (/) followed by the mutant allele.

(B) Immunocytochemistry of FUS protein revealing its subcellular localization in iPSCs of different genotypes. To better visualize the cytoplasmic compartment, iPSCs were single-cellularly dissociated and treated with ROCK inhibitor Y-27632 which causes cells to stretch out on the culture surface.

(C) aCGH and SNP microarray results of iPSC clones with WT and P525L Hom genotypes. Balanced red and blue aCGH signals centered at 0 copy number indicate no gross karyotypic abnormalities such as large genomic sequence amplications or deletions. Balanced distribution of green SNP signals across 0, 1, 2 copy numbers denotes normal SNP distributions. Shaded green region with SNP signals missing from 1 copy number signify CN-LOH across entire chromosome arm.

(D) As a technical note, we report that the Abcam antibody seemed to recognize only WT FUS but not P525L whereas the Proteintech antibody recognized both protein isoforms. The immunogen for the Abcam antibody is amino acids 1-50 of human FUS whereas that for the Proteintech antibody is amino acids 52-400 of human FUS. We hypothesize that P525L changes the 3-dimensional structure of FUS is a way that renders the Abcam antibody epitope unrecognizable but does not affect that of Proteintech.

Scale bar = 50 μm.

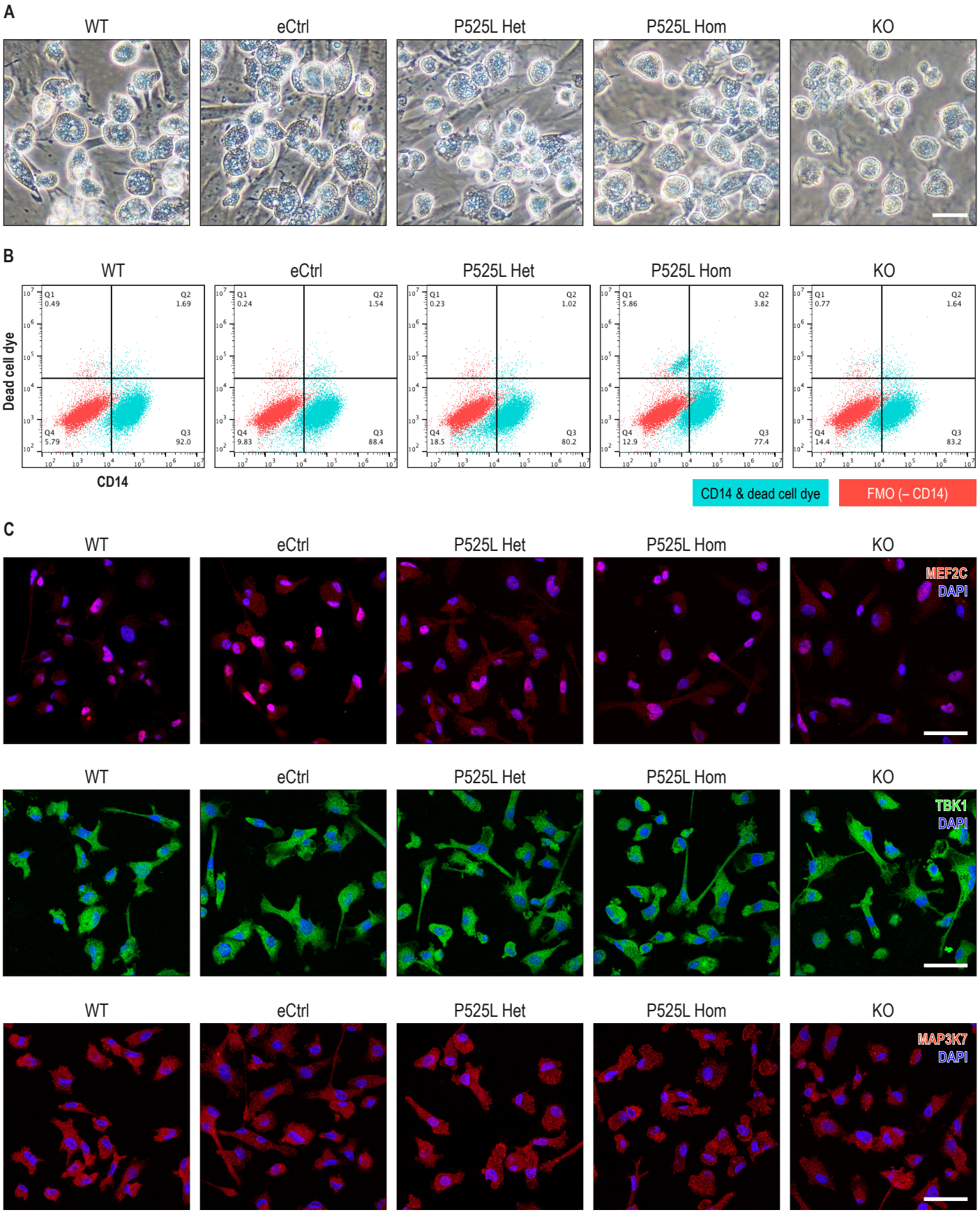
A
WT
eCtrl
P525L Het
P525L Hom
KO
B
WT
eCtrl
P525L Het
P525L Hom
KO
Dead cell dye
CD14
Q1 0.49
Q2 1.69
Q4 5.79
Q3 92.0
Q1 0.24
Q2 1.54
Q4 9.83
Q3 88.4
Q1 0.23
Q2 1.02
Q4 18.5
Q3 80.2
Q1 5.86
Q2 3.82
Q4 12.9
Q3 77.4
Q1 0.77
Q2 1.64
Q4 14.4
Q3 83.2
CD14 & dead cell dye
FMO (– CD14)
C
WT
eCtrl
P525L Het
P525L Hom
KO
MEF2C
DAPI
TBK1
DAPI
MAP3K7
DAPI

Figure S2. Differentiation of human iPSC lines with *FUS* P525L mutations and isogenic controls into MIGs. Related to Figure 2.

(A) Phase contrast images of iPSC-derived myeloid progenitor cells of different *FUS* genotypes.

(B) Flow cytometry dot plots of characteristic myeloid progenitor surface marker CD14 as well as a dead cell dye to indicate viability in myeloid progenitor cells. FMO: fluorescence minus one control using WT cells.

(C) Immunocytochemistry of additional microglia proteins in iPSC-derived MIGs of different *FUS* genotypes.

Scale bar = 50 μm. Presented here are clones from the AG line.

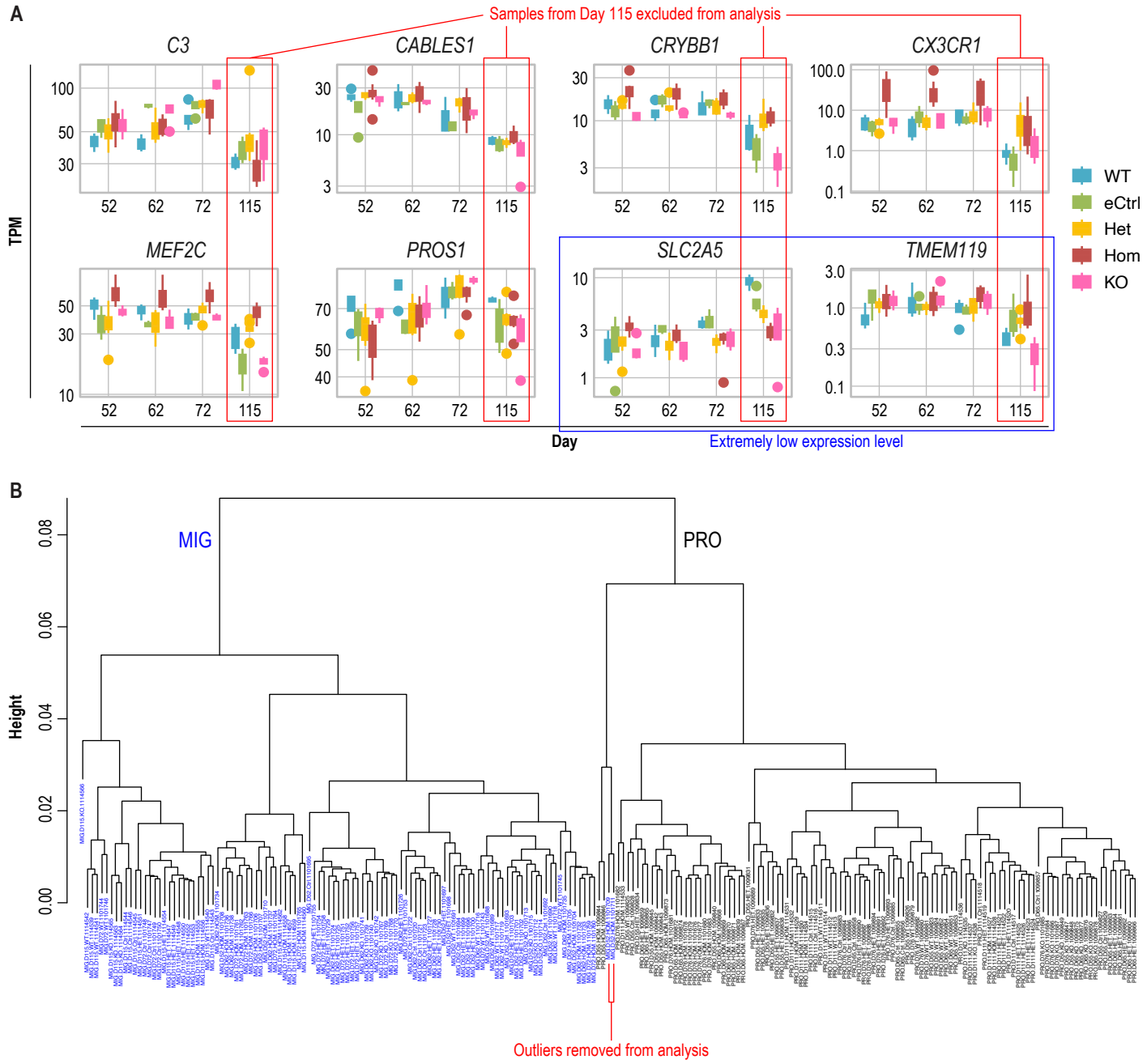
A
Samples from Day 115 excluded from analysis
C3
CABLES1
CRYBB1
CX3CR1
MEF2C
PROS1
SLC2A5
TMEM119
TPM
Day
Extremely low expression level
WT
eCtrl
Het
Hom
KO
B
MIG
PRO
Height
Outliers removed from analysis

Figure S3. Identity validation via RNA sequencing of iPSC-derived MIGs with *FUS* P525L mutations and isogenic controls. Related to Figure 3.

(A) Box plots of gene expression level of microglial markers in MIGs across genotypes and time points at which myeloid progenitors were harvested for terminal differentiation. TPM: transcript per million. Presented here are clones from the AG line.

(B) Hierarchical clustering of transcriptome profiles from RNA-seq of MIGs and their preceding PROs. The two outlier samples here are the same as those in the PCA plot (**Figure 3A** and **3B**).

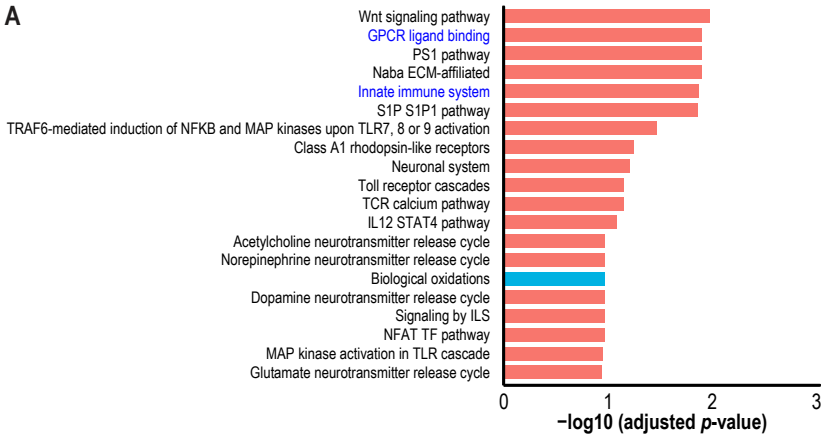
A
Wnt signaling pathway
GPCR ligand binding
PS1 pathway
Naba ECM-affiliated
Innate immune system
S1P S1P1 pathway
TRAF6-mediated induction of NFKB and MAP kinases upon TLR7, 8 or 9 activation
Class A1 rhodopsin-like receptors
Neuronal system
Toll receptor cascades
TCR calcium pathway
IL12 STAT4 pathway
Acetylcholine neurotransmitter release cycle
Norepinephrine neurotransmitter release cycle
Biological oxidations
Dopamine neurotransmitter release cycle
Signaling by ILS
NFAT TF pathway
MAP kinase activation in TLR cascade
Glutamate neurotransmitter release cycle
0
1
2
3
−log10 (adjusted p-value)

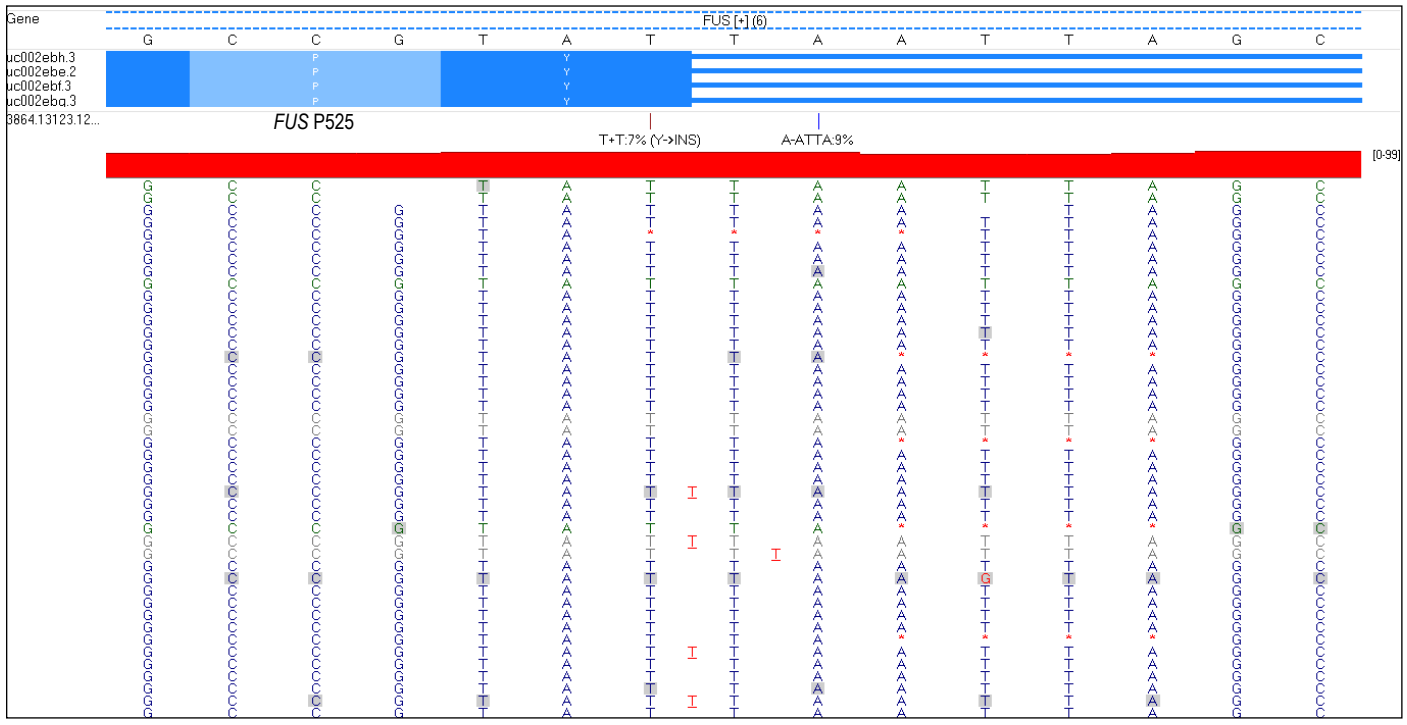
B
Gene
FUS [+] (6)
G C C G T A T T A A T T A G C
uc002ebh.3
uc002ebe.2
uc002ebf.3
uc002ebg.3
3864.13123.12...
FUS P525
T+T:7% (Y->INS)
A-ATTA:9%
[0-99]

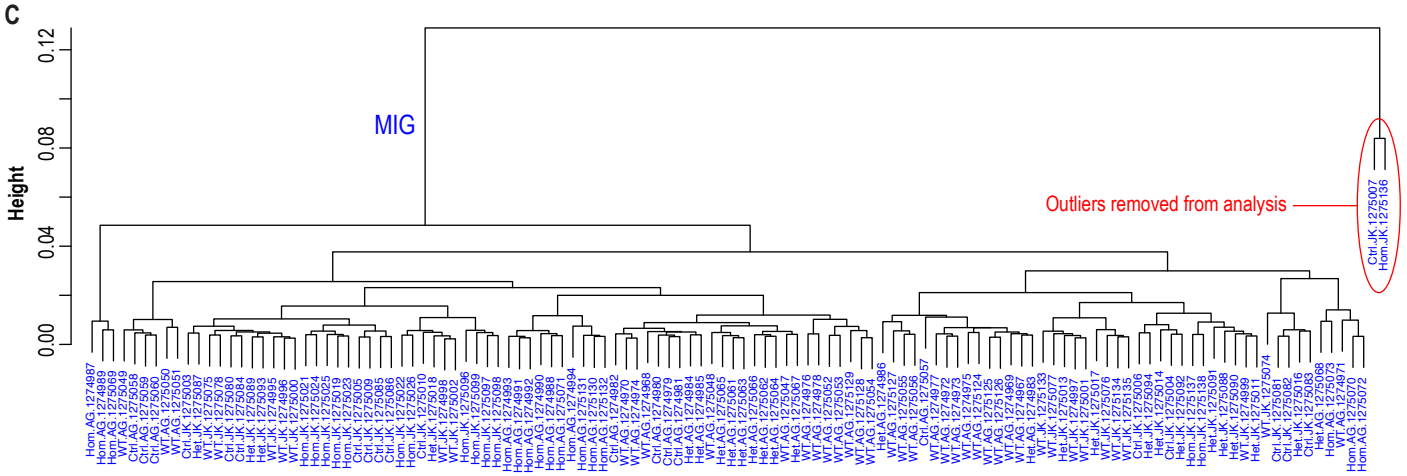
C
Height
0.12
0.08
0.04
0.00
MIG
Outliers removed from analysis
Ctrl.JK.1275097
Hom.JK.1275156

Figure S4. Homozygous *FUS* P525L MIGs display transcriptional perturbations of genes associated with characteristic microglial functions. Related to Figure 4.

(A) Top 20 MSigDB Canonical Pathways terms associated with genes enriched in the P525L Hom signature. Terms in blue are linked to characteristic features and functions of microglia. Red bars indicate that the majority of Hom signature genes associated with a term is upregulated; blue bars indicate the majority is downregulated. Multiple testing correction was performed using the Benjamini-Hochberg procedure to obtain adjusted *p*-values. See **Table S1** for more gene enrichment analysis results.

(B) Screenshot of RNA-seq reads aligned to the *FUS* locus for one of the JK WT MIG samples. A small percentage (11.9% ± 5.7%) of reads has a T insertion right after the last amino acid-coding codon which does not alter the FUS WT amino acid sequence but does extend the protein by 40 amino acids. Another small percentage of reads has an ATTA deletion within the stop codon (TAA) that simply reconstituted another stop codon (TAG) at the exact position. We deduced that our iPSC JK WT line was contaminated with cells harboring undesired CRISPR mutations and was hence not clonal.

(C) Hierarchical clustering of RNA-seq transcriptome profiles of MIGs differentiated from AG and JK lines with various *FUS* genotypes. The two outlier samples here are the same as two of those in the PCA plot (**Figure 4B**).

A

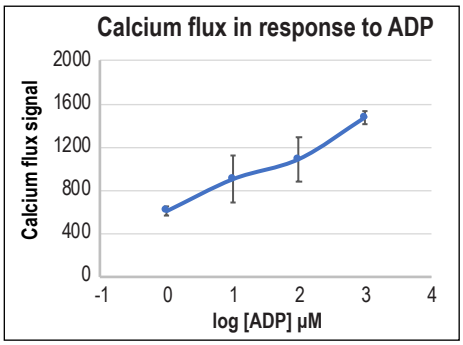
Calcium flux in response to ADP
Calcium flux signal
2000
1600
1200
800
400
0
-1
0
1
2
3
4
log [ADP] µM

B

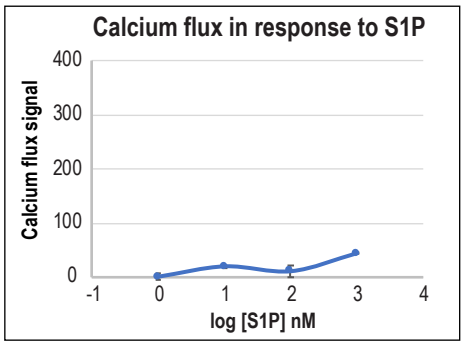
Calcium flux in response to S1P
Calcium flux signal
400
300
200
100
0
-1
0
1
2
3
4
log [S1P] nM

C

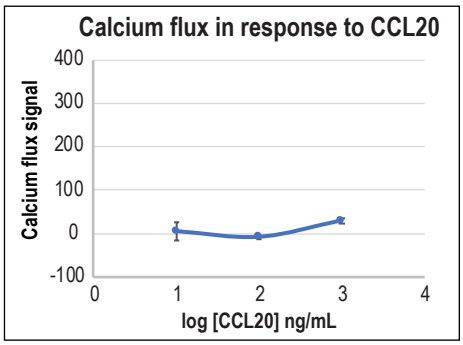
Calcium flux in response to CCL20
Calcium flux signal
400
300
200
100
0
-100
0
1
2
3
4
log [CCL20] ng/mL

D

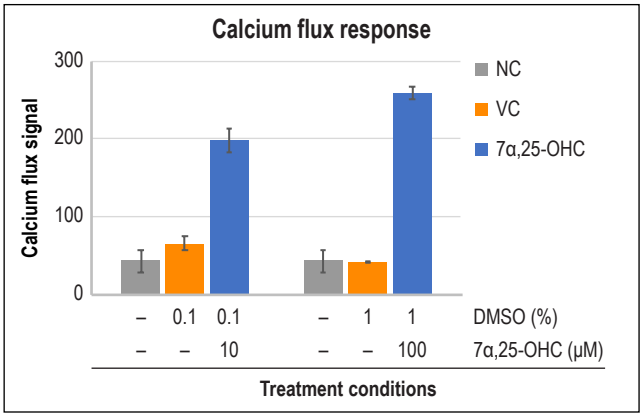
Calcium flux response
Calcium flux signal
300
200
100
0
NC
VC
7α,25-OHC
– 0.1 0.1 – 1 1
DMSO (%)
– – 10 – – 100
7α,25-OHC (µM)
Treatment conditions

Figure S5. Differentially expressed chemoreceptor genes in MIGs with *FUS* P525L mutations lead to perturbations of ligand-induced intracellular calcium signaling. Related to Figure 5.

(A, B, C) Intracellular calcium response to increasing concentrations of **(A)** ADP as positive control, **(B)** S1P, or **(C)** CCL20 in MIGs.

(D) Intracellular calcium response to 7α,25-OHC compared to the DMSO vehicle control (VC) and assay buffer-only negative control (NC) in MIGs.

Error bars represent standard deviation across two replicate wells in the JK line; $n = 2$. Datasets herein were not normalized to their Euclidean distance.

A

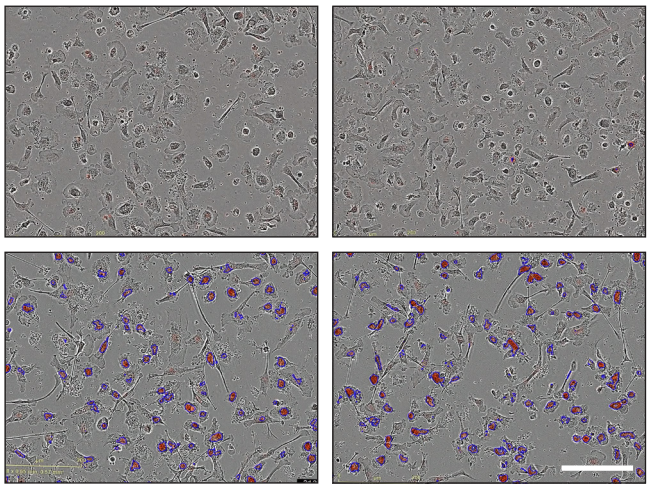

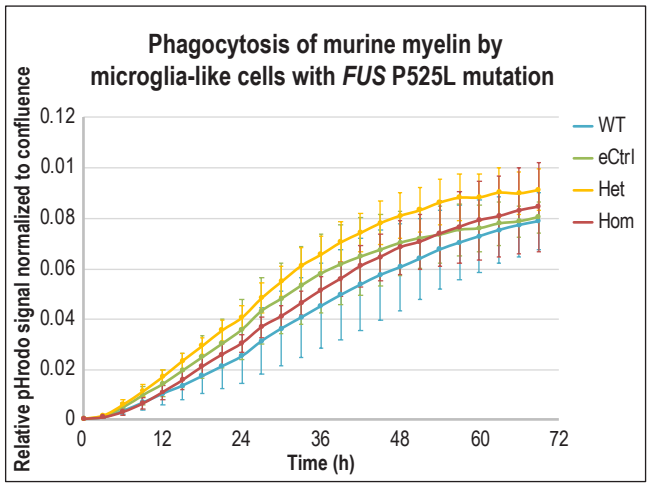

B

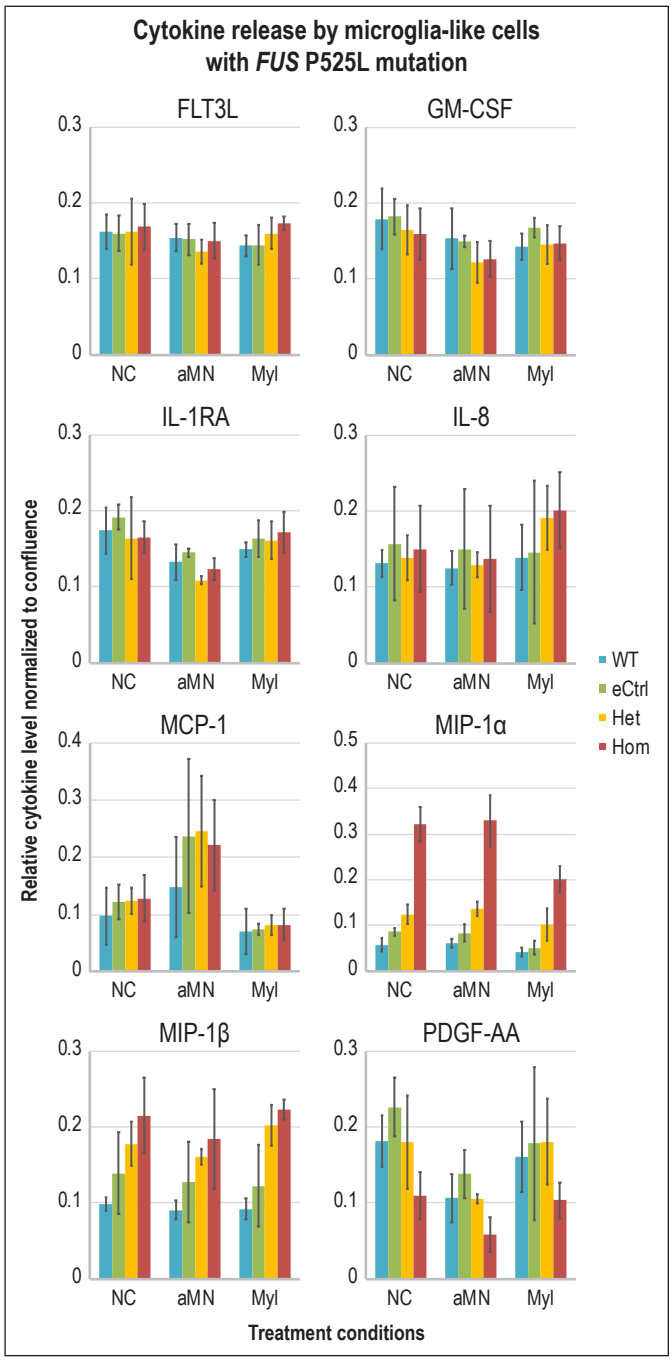

C

	G-CSF	GM-CSF	GRO-α	GRO-β	IL-1β
NC_6h	0.00	0.00	0.00	0.00	0.00
NC_24h	0.00	-1.16	0.00	0.00	0.00
NC_72h	0.00	2.18	0.00	0.00	0.05
aNeu_6h	0.11	-1.95	0.00	0.00	0.12
aNeu_24h	0.59	-1.96	0.00	0.00	0.00
aNeu_72h	0.36	1.72	0.00	0.00	0.00
Eco_6h	0.00	-0.62	0.00	0.00	1.90
Eco_24h	0.97	0.34	0.00	0.17	5.67
Eco_72h	5.42	3.38	2.32	3.99	6.02

	IL-1ra	IL-2	IL-6	IL-8	IL-10	IP-10	MCP-1	MIP-1α	MIP-1β	PDGF-AA	RANTES	TNF-α
NC_6h	0.00	0.00	0.00	0.00	0.00	0.00	0.00	0.00	0.00	0.00	0.00	0.00
NC_24h	1.11	0.00	-0.06	0.01	-0.37	0.00	0.00	0.00	0.00	0.00	-0.16	0.00
NC_72h	2.11	0.06	-0.09	2.94	-0.13	0.07	1.73	0.00	0.00	0.26	-0.16	0.00
aNeu_6h	0.40	0.00	0.00	-0.40	-0.23	0.00	0.00	0.00	0.00	0.06	-0.16	0.00
aNeu_24h	1.06	0.00	-0.09	0.14	-0.54	0.00	0.00	0.00	0.00	0.15	0.00	0.00
aNeu_72h	1.54	0.00	-0.04	3.21	-0.43	0.07	3.30	0.00	0.00	0.06	-0.10	0.00
Eco_6h	1.21	0.09	3.90	4.79	-0.13	0.00	0.00	3.14	0.61	0.18	0.05	5.22
Eco_24h	2.79	1.29	7.32	8.39	1.50	0.00	3.74	6.21	2.80	0.00	-0.05	6.81
Eco_72h	5.06	3.43	10.86	11.90	4.69	1.08	9.38	7.72	6.55	1.68	1.27	9.10

Figure S6. MIGs with *FUS* P525L mutations do not exhibit phagocytosis or cytokine release phenotypes. Related to Figure 6.

(A) Top half of panel: Phase contrast and red fluorescence overlay images of MIGs. Red fluorescence represents phagocytosed pHrodo-conjugated murine myelin while blue outline masks indicate signals above background. pHrodo is a pH-sensitive dye that is almost non-fluorescent at neutral pH but fluoresces brightly in acidic environments such as phagosomes. Due to space constraint, only representative images of WT and *FUS* P525L Hom cells are displayed. Scale bar = 200 μm. Bottom half of panel: Graph for phagocytosis signal normalized to cell confluence versus time from live imaging of MIGs with different *FUS* genotypes engulfing pHrodo-conjugated myelin. Error bars represent standard deviation across both AG and JK lines, each with at least three replicate wells; $n \geq 6$.

(B) Level of cytokine in cell culture supernatant released by MIGs under different treatment conditions after 72 h. NC: untreated negative control; aMN: apoptotic motor neurons; Myl: murine myelin. Presented here are cytokines that were above the detection limit of the immunoassay. Error bars represent standard deviation across both AG and JK lines, each with at least three replicate wells; $n \geq 6$.

(C) Cytokine level change in culture supernatant of MIGs under different treatment conditions after 6 h, 24 h, or 72 h. NC: untreated negative control; aNeu: apoptotic neurons; Eco: *E.coli*. Cytokine level in each condition was compared to that in NC at 6 h for the respective cytokine and reported as log2 fold-change (+/- mode). Only cytokines with log2 fold-change magnitude greater than 1 were shown. Presented here is the AG line with three replicate wells per condition.

Table S1: ***FUS*** **signature genes and their expression level fold-changes**

Table S2: **GO- and MSigDB Canonical Pathways-linked enriched genes in** ***FUS*** **P525L Hom signature.**

Table S3: **RT-qPCR of selected** ***FUS*** **P525L Hom signature genes**

Table S4: **Actively expressed microglia-enriched genes in primary human microglia and MIGs**

Movie S1. **Morphological and motile features of human iPSC-derived MIGs with homozygous FUS P525L mutations and isogenic control. Related to Figure 2.**

(A, B) Time-lapse movie of *FUS* (A) eCtrl and (B) P525L Hom MIGs. Phase contrast images were taken every 30 s over a period of 20 min; video speed increased 300 times. Presented here are clones from the AG line.

SUPPLEMENTAL EXPERIMENTAL PROCEDURES

Derivation of human iPSC lines

The human iPSC AG line was derived from male FibroGRO Xeno-Free Human Foreskin Fibroblasts (Sigma-Aldrich, Cat. #: SCC058) while the JK line was derived from male Neonatal Human Foreskin Fibroblasts (GlobalStem, Cat. #: GSC-3002). Both fibroblast lines were independently reprogrammed using the Simplicon RNA Reprogramming Kit (Sigma-Aldrich, Cat. #: SCR550) based on manufacturer's protocol. In brief, fibroblast cells were liposomally transfected with synthetic, self-replicating, non-integrating, polycistronic RNA transcripts encoding the reprogramming factors OCT-4, KLF-4, SOX-2, and GLIS1 as well as a puromycin resistance gene. B18R, encoded in co-transfected RNA transcripts and supplemented as proteins in cell culture media, was delivered to inhibit the cellular interferon response-mediated depletion of exogenous RNA. Transfected cells were then positively selected based on puromycin resistance before selectively degrading the transfected RNA by B18R withdrawal. Successful derivation of iPSCs were confirmed by checking for the expression of the pluripotency markers OCT-4, SOX2, NANOG, TRA-1-60, and TRA-1-81 via immunocytochemistry.

All iPSC lines were maintained on Geltrex Basement Membrane Matrix (Gibco, Cat. #: A1413301) in StemFlex medium (Gibco, Cat. #: A3349401) without antibiotics; incubated at 37ºC, 5% CO_2, and atmospheric O_2 level; and routinely passaged as cell clusters with ReLeSR (STEMCELL Technologies, Cat. #: 05872).

CRISPR engineering of iPSC lines

To genetically modify the *FUS* gene locus, CRISPR reagents were delivered into iPSCs by electroporation using the Neon Transfection System (Invitrogen, Cat. #: MPK5000S) according to manufacturer's protocol. Briefly, iPSCs were dissociated with TrypLE Select Enzyme (Gibco, Cat. #: 12563011) and $1x10^5$ cells were combined in 10 µL of Buffer R with 30 pmol of TrueCut Cas9 Protein v2 (Invitrogen, Cat. #: A36498), 30 pmol of each Alt-R CRISPR-Cas9 sgRNA (custom-made by Integrated DNA Technologies, Iowa, USA), and, when repair templates were required, 10 pmol of each ssODN (custom-made by Integrated DNA Technologies, Iowa, USA). The reaction mixture was then electroporated using the parameters 1300 V, 10 ms, and 3 pulses, before plating the cells on Geltrex matrix in StemFlex media supplemented with CloneR (STEMCELL Technologies, Cat. #: 05888) to increase single-cell survival. When recovered cells reached 75% confluence, they were dissociated into a single-cell suspension, seeded at a low density of 30 cells/cm^2, and cultured to form clonal colonies. Independent iPSC clones were then picked, screened for successful CRISPR modification using PCR and Sanger sequencing (service provided by Genewiz, New Jersey, USA), and checked to ensure no gross karyotypic and genomic abnormalities via aCGH and SNP microarray (services provided by Cell Line Genetics, Wisconsin, USA).

For generating the KO, two flanking sgRNAs with these target sequences were designed: Upstream, 5'-CTCCAGGCGTCGGTACTCAG-3'; Downstream, 5'-GAACTGGAATACAGTGTTCG-3'. For the other genotypes with point mutations, an sgRNA with this target sequence: 5'-GGGAGCCAGGCTAATTAATA-3', and the following ssODN repair templates were designed: P525L, 5'-TACTTAATTTTTTTTTTTTTTTTTGCAGGGGTGAGCACAGACAGGATCGCAGGGAGAGGCTGTATTAATTAGCCTGGCTCCCCAGGTTCTGGAACAGCTTTTTGTCCTGTACCCAGTGTTA-3'; eCtrl, 5'-TACTTAATTTTTTTTTTTTTTTTTTGCAGGGGTGAGCACAGACAGGATCGCAGGGAGAGGCCGTACTGATTAGCCTGGCTCCCCAGGTTCTGGAACAGCTTTTTGTCCTGTACCCAGTGTTA-3'.

Directed differentiation of human iPSCs into MIGs

Human iPSCs were directedly differentiated into MIGs based on the protocol from Douvaras *et al*. (2017)[1] with a few modifications. All differentiation factor proteins were procured from R&D Systems and all cell cultures were incubated at 37ºC, 5% CO_2, and atmospheric O_2 level. In brief, iPSC colonies were cut into square pieces using StemPro EZPassage Disposable Stem Cell Passaging Tool (Gibco, Cat. #: 23181010) and seeded at a density of 2.5 pieces/cm^2 on Matrigel Basement Membrane Matrix (Corning, Cat. #: 356231) in mTeSR1 medium (STEMCELL Technologies, Cat. #: 85850) containing 10 µM ROCK inhibitor Y-27632 (Tocris, Cat. #: 1254). The next day, medium was replaced with fresh mTeSR1. Three days post-seeding (Day 0), differentiation was initiated by applying 80 ng/ml BMP-4 (Cat. #: PRD314) in mTeSR1 for 4 days. On Day 4, medium was switched to StemPro-34 SFM (Gibco, Cat. #: 10639011)

containing 25 ng/ml bFGF (Cat. #: PRD233), 100 ng/ml SCF (Cat. #: PRD255), 80 ng/ml VEGF (Cat. #: PRD293), and 2 mM GlutaMAX Supplement (Gibco, Cat. #: 35050061) for 2 days. Henceforth, all media were supplemented with 2 mM GlutaMAX. On Day 6 and 10, media were replaced with StemPro-34 containing 50 ng/ml FLT3L (Cat. #: PRD308), 50 ng/ml IL-3 (Cat. #: PRD203), 50 ng/ml M-CSF (Cat. #: PRD216), 50 ng/ml SCF, and 5 ng/ml TPO (Cat. #: 288-TP) for 4 days respectively. From Day 14 onwards, every 3 to 4 days, media were replaced with StemPro-34 containing 50 ng/ml FLT3L (Cat. #: 308-FK-MTO), 25 ng/ml GM-CSF (Cat. #: 215-GM-MTO), and 50 ng/ml M-CSF (Cat. #: 216-MC-MTO).

Between Day 55 and 74, every 3 to 4 days, myeloid progenitor cells in the supernatant were harvested and plated at a density of $5x10^4$ cells/cm^2 on Laminin-521 (Gibco, Cat. #: A29248) in RPMI 1640 medium (Gibco, Cat. #: 11875093) supplemented with 10 ng/ml GM-CSF and 100 ng/ml IL-34 (Cat. #: 5265-IL-MTO) to be further differentiated into MIGs for 2 weeks. This microglia medium was also used for cell maintenance and refreshed every 3 to 4 days. MIGs were harvested using StemPro Accutase Cell Dissociation Reagent (Gibco, Cat. #: A1110501) and cryopreserved in CryoStor CS10 Freeze Media (BioLife Solutions, Cat. #: 210102) based on manufacturer's protocol. Cryopreserved MIGs were validated to be highly similar to their non-cryopreserved counterpart in terms of our *FUS* P525L Hom signature phenotype (**Table S3**).

Immunocytochemistry and confocal microscopy

Cells were cultured on 8-well chamber slides, fixed with 4% formaldehyde (Electron Microscopy Sciences, Cat. #: 15714-S) in PBS at room temperature (RT) for 15 min, and simultaneously permeabilized and blocked with 5% donkey serum (Jackson Immunoresearch, Cat. #: 017-000-121) and 0.2% Triton X-100 in PBS at RT for 1 hr. Primary antibody staining was performed at 4°C overnight and secondary antibody staining at RT for 1 hr, both in the permeabilization and blocking buffer. Three washes with PBS were performed after each antibody incubation step. Immunostained cells were subsequently mounted with Fluoromount-G Mounting Medium with DAPI (Invitrogen, Cat. #: 00-4959-52). Images were acquired under the Zeiss LSM 780 confocal microscope with the ZEN Black software and processed using the ImageJ software [2].

The following primary antibodies were used at the specified dilution: rabbit anti-FUS at 1:500 (Proteintech, Cat. #: 11570-1-AP; Abcam, Cat. #: ab84078), rabbit anti-MAP3K7 at 1:500 (Abcam, Cat. #: ab109526), mouse anti-MEF2C at 1:200 (Novus Biologicals, Cat. #: NBP2-00493), rabbit anti-TBK1 at 1:100 (Abcam, Cat. #: ab40676), and goat anti-TREM2 at 1:100 (R&D Systems, Cat. #: AF1828). The following donkey secondary antibodies from Invitrogen were used at 1:500 dilution: Alexa Fluor 488 anti-goat IgG (Cat. #: A11055), Alexa Fluor 555 anti-mouse IgG (Cat. #: A31570), Alexa Fluor 488 anti-rabbit IgG (Cat. #: A21206), and Alexa Fluor 555 anti-rabbit IgG (Cat. #: A31572).

Flow cytometry

Harvested cells were resuspended in PBS with LIVE/DEAD Fixable Near-IR Dead Cell Stain (Invitrogen, Cat. #: L10119) at 1:1000 dilution, incubated on ice for 15 min, washed with PBS, and centrifuged at 400 g for 2 min before aspirating supernatant. Pelleted cells were resuspended in PBS with 5% fetal bovine serum (FBS) (Gemini Bio, Cat. #: 100-500), Human BD Fc Block (BD Biosciences, Cat. #: 564219) at 1:20 dilution, and fluorophore-conjugated antibodies. Cells were incubated on ice for 20 min, washed using PBS with 5% FBS, and pelleted by centrifugation. Stained cells were then fixed by being resuspended in PBS with 2% formaldehyde and incubated at RT for 15 min, before being passed through the cap strainer of flow cytometry tubes (Corning, Cat. #: 352235). Whenever possible, cell samples and reagents were shielded from light and kept cold on ice. Flow cytometry was performed on the Beckman Coulter CytoFLEX LX machine using the CytExpert software and acquired data were analyzed using the FlowJo software.

The following fluorophore-conjugated antibodies were procured from BioLegend and used at 1:20 dilution unless otherwise stated: Alexa Fluor 488 anti-CD14 (Cat. #: 325610), Brilliant Violet 421 anti-CX3CR1 (Cat. #: 341620), Alexa Fluor 647 anti-MERTK (Cat. #: 367606), Brilliant Violet 605 anti-MRC1 (Cat. #: 321140), and PE anti-P2RY12 at 1:800 dilution (Cat. #: 392104).

RNA sequencing

Cells were homogenized in TRIzol (Invitrogen, Cat. #: 15596026) and chloroform was used for phase separation. The aqueous phase, containing total RNA, was purified using MagMAX-96 for Microarrays Total RNA Isolation Kit (Applied Biosystems, Cat. #: AM1839) and genomic DNA was

removed using RNase-free DNase Set (Qiagen, Cat. #: 79256). The mean RNA Quality Number (RQN) of all our samples was 9.43 ± 0.03. Strand-specific RNA-seq libraries were prepared from 500 ng of RNA using KAPA Stranded mRNA-Seq Kit (KAPA Biosystems, Cat. #: KK8401) and amplified by 12-cycle PCR. Sequencing was performed on the Illumina HiSeq 2000 Sequencing System by multiplexed paired-read run with 100 cycles. The resulting FASTQ files were analyzed via the FastQC software to ensure sufficient data quality. Subsequently, sequencing reads were mapped to the human genome (hg19) using the OmicSoft ArrayStudio software with two mismatches allowed. Across all our samples, the median of uniquely mapped paired reads was 86.09%.

All samples in the large dataset from which the differential gene expression analysis was performed were sequenced in the same batch to eliminate technical covariates. For quality control, the mean of the following parameters was obtained: Total Reads: $5.27 \times 10^7 \pm 7.90 \times 10^5$, Reads Mapped in Pair: 96.34% ± 0.10%, Reads Mapped to Gene: 90.60% ± 0.15%, Reads Mapped to Exon: 53.48% ± 0.14%, Reads Mapped to Exon Junction: 27.36% ± 0.09%, Reads Mapped to Intron: 9.76% ± 0.10%, Reads Mapped to rRNA: 3.61% ± 0.07%, Reads Mapped to Intergenic Region: 9.40% ± 0.15%.

Global similarity of samples based on RNAseq results was assessed via principal component analysis and hierarchical clustering. Based on the guidance described by Iglewicz and Hoaglin (1993)[3], z-score-based outlier detection was conducted for all sample sets shown in **Figure 3A**, **3B**, and **4B**. Each sample was projected onto the first two principal components. Next, the Euclidean distance between each sample and the mean of all samples (a.k.a. the centroid of all samples) was computed, and subsequently converted to a z-score by subtracting the mean distance and then dividing the difference by the standard deviation of the distances. Samples with an absolute z-score equal or greater than 3.5 were defined as outliers. The abnormality of the outlier samples was consistently supported by the observation that two outlier microglia samples wrongly clustered with progenitor samples in the pilot dataset (**Figure S3B**), and two outlier samples formed an isolated branch away from all other microglia samples in the hierarchical clustering of the large dataset (**Figure S4C**). The third outlier sample in the large dataset was flagged as an outlier due to its abnormal fibroblast-like morphology, prior to and independent of RNA-seq data analysis. These abnormal outliers were removed to ensure a high quality of the samples used in our analyses.

Reverse transcription-quantitative PCR

Messenger RNA from purified total RNA described above was reverse-transcribed into cDNA using SuperScript VILO Master Mix (Invitrogen, Cat. #: 11755500). The resulting cDNA was then amplified and quantified with the SensiFAST Probe Lo-ROX Kit (Meridian Bioscience, Cat. No: BIO-84050) using the QuantStudio 12K Flex Real-Time PCR System. An endogenous control gene (*ACTB*) was used to normalize any cDNA input differences. Data were reported via the comparative C_T (threshold cycle) method [4].

Intracellular calcium flux assay

Experimental parameters for the FLIPR Tetra High-throughput Cellular Screening System with ICCD Camera were set up as such: Exposure: 0.53 s, Camera Gain: 2000, Camera Gate: 6%, Addition Volume: 50 µL, Compound Concentration: 5-fold, Excitation LED: 470-495 nm, Emission Filter: 515-575 nm, LED Intensity: 30%, Addition Height: 225 µL, Tip Up Speed: 10 mm/s, Addition Speed: 10 µL/s. Using the Screenworks software, raw data were acquired as Relative Fluorescence Units (RFU) and processed by applying the kinetic reduction type of Max-Min across the entire acquisition period to obtain intracellular calcium flux signal values.

The following chemoreceptor ligands from Sigma-Aldrich were used: UDP (Cat. #: 94330), 7α,25-OHC (Cat. #: SML0541), S1P (Cat. #: 73914), CCL20 (Cat. #: SRP4491), and ADP (Cat. #: A2754); whereas the following chemoreceptor inhibitors were applied: MRS2578 (Cat. #: M0319) and NIBR189 (Cat. #: SML1981). In terms of solvents, 7α,25-OHC, MRS2578, and NIBR189 were dissolved in DMSO (Sigma-Aldrich, Cat. #: D2650); S1P in 0.3 M NaOH; and the other chemicals in ddH_2O. DMSO itself did not significantly elicit an intracellular calcium response in MIGs (**Figure S5D**).

Live-cell imaging for phagocytosis assays

MIGs were plated at 1×10^4 cells per well into flat-clear-bottom black-walled tissue culture-treated 96-well plates (Corning, Cat. #: 3904). At least 1 day later, assay dye reagent (as detailed below) was added. The plates were transferred into the Sartorius IncuCyte S3 Live-Cell Analysis System housed

within an incubator at 37ºC, 5% CO_2, and atmospheric O_2 level until the end of the assay. Nine tiled images per well from three replicate wells were taken every 3 hr for 72 hr using the 20X objective lens with phase contrast and red fluorescence acquisition at 400 ms of exposure. Data analysis was performed using the IncuCyte software to quantify the assay dye's red fluorescence signal in terms of integrated intensity as well as cell amount based on confluence for normalization.

Specific details for each following assay are further provided. (A) Apoptotic motor neuron efferocytosis assay: From the iCell Motor Neurons Kit (FUJIFILM Cellular Dynamics, Cat. #: 01279), $3.8x10^5$ human iPSC-derived motor neurons were seeded into a well of a clear tissue culture-treated 12-well plate and cultured for at least 1 week according to manufacturer's protocol. Motor neurons were then irradiated at 100 Jm^{-2} to induce apoptosis. Three days later, apoptotic motor neurons were dislodged by pipetting, harvested, and conjugated with pHrodo dye at a final concentration of 1 µg/mL using the IncuCyte pHrodo Red Cell Labeling Kit for Phagocytosis (Sartorius, Cat. #: 4649) based on manufacturer's protocol. In the last step, pHrodo-conjugated apoptotic motor neurons were resuspended in 5 mL of microglia medium and 100 uL per well of this suspension were used in the assay. (B) Myelin phagocytosis assay: Myelin was obtained from 3-month old C57BL/6 mouse brain as described in Larocca and Norton (2007) with minor modifications. In principle, brain tissue was homogenized in isotonic sucrose solution, followed by a cycling series of density gradient and differential centrifugation steps to isolate myelin membranes. Purified myelin was quantified based on protein content, adjusted to 1 mg/mL in PBS, triturated with an insulin syringe (BD, Cat. #: 328411), and labeled with 10 µg/mL pHrodo iFL Red STP Ester (Invitrogen, Cat. #: P36010) at RT for 45 min in the dark. Following centrifugation at 4000 g for 10 min, supernatant with unreacted dye was removed before resuspending myelin pellet in PBS. For the assay, approximately 1 ug per well of pHrodo-conjugated murine myelin was applied.

Cytokine profiling multiplex immunoassay

Cell culture supernatants from phagocytosis assays were gently collected without touching adherent cells at the desired time points. Released cytokines were then profiled using either the Human XL Cytokine Magnetic Luminex Performance Assay 45-plex Fixed Panel (R&D Systems, Cat. #: LKTM014) or the MILLIPLEX MAP Human Cytokine/Chemokine/Growth Factor Panel A 48 Plex Premixed Magnetic Bead Panel (Millipore, Cat. #: HCYTA-60K-PX48) according to manufacturer's protocol. In brief, supernatants from our experiments and cytokine concentration standards from the kit were incubated with a mixture of distinctly color-coded magnetic beads where each color encodes for specific capture antibodies against a particular cytokine target. Next, biotinylated detection antibodies against the capture antibodies were introduced before being reacted with fluorophore-conjugated streptavidin which serves as the reporter molecule. All washes to remove excess reagents were facilitated by immobilizing the beads with a handheld magnet. Identification and quantification of cytokines on the beads were then performed using the flow cytometry-based Luminex FLEXMAP 3D instrument with the xPONENT software. Acquired data were analyzed via the Millipore Belysa software to construct concentration standard curves from which absolute amounts of cytokine were inferred. We note that the assay performances of both commercial kits were very similar.

Statistical analysis for functional assays

For calcium assays, live-cell imaging, and cytokine profiling experiments, the dataset for each independent line in each experimental repeat (where applicable) was normalized by simple division with its Euclidean distance (square root of sum of squares of each data point). Within each *FUS* genotype, the normalized data points were then averaged across independent lines and experimental repeats (where applicable). Statistical analyses were performed using the unpaired *t*-test (one-tailed) on each of the other genotypes compared to WT. For RT-qPCR experiments, the paired *t*-test (one-tailed) was performed on P525L Hom compared to WT. Quantitative differences with $p < 0.05$ were considered significant.

SUPPLEMENTAL REFERENCES

1. Douvaras P, Sun B, Wang M, Kruglikov I, Lallos G, Zimmer M, *et al*. Directed Differentiation of Human Pluripotent Stem Cells to Microglia. Stem Cell Reports. 2017;8(6):1516-24.
2. Schneider CA, Rasband WS, Eliceiri KW. NIH Image to ImageJ: 25 years of image analysis. Nat Methods. 2012;9(7):671-5.
3. Iglewicz BH, D. C. How to detect and handle outliers. Milwaukee, Wisconsion: ASQC Quality Press; 1993.
4. Schmittgen TD, Livak KJ. Analyzing real-time PCR data by the comparative C(T) method. Nat Protoc. 2008;3(6):1101-8.
5. Larocca JN, Norton WT. Isolation of myelin. Curr Protoc Cell Biol. 2007;Chapter 3:Unit3 25.
6. Wagner GP, Kin K, Lynch VJ. A model based criterion for gene expression calls using RNA-seq data. Theory Biosci. 2013;132(3):159-64.